

1-1-2014

## Synthesis and X-ray powder diffraction, electrochemical, and genotoxic properties of a new azo-Schiff base and its metal complexes

MUSTAFA BAL

GÖKHAN CEYHAN


BARIŞ AVAR

MUHAMMET KÖSE

AHMET KAYRALDIZ

*See next page for additional authors*

Follow this and additional works at: <https://journals.tubitak.gov.tr/chem>

 Part of the [Chemistry Commons](#)

---

### Recommended Citation

BAL, MUSTAFA; CEYHAN, GÖKHAN; AVAR, BARIŞ; KÖSE, MUHAMMET; KAYRALDIZ, AHMET; and KURTOĞLU, MÜKERREM (2014) "Synthesis and X-ray powder diffraction, electrochemical, and genotoxic properties of a new azo-Schiff base and its metal complexes," *Turkish Journal of Chemistry*. Vol. 38: No. 2, Article 6. <https://doi.org/10.3906/kim-1306-28>

Available at: <https://journals.tubitak.gov.tr/chem/vol38/iss2/6>

This Article is brought to you for free and open access by TÜBİTAK Academic Journals. It has been accepted for inclusion in Turkish Journal of Chemistry by an authorized editor of TÜBİTAK Academic Journals. For more information, please contact [academic.publications@tubitak.gov.tr](mailto:academic.publications@tubitak.gov.tr).

---

## Synthesis and X-ray powder diffraction, electrochemical, and genotoxic properties of a new azo-Schiff base and its metal complexes

### Authors

MUSTAFA BAL, GÖKHAN CEYHAN, BARIŞ AVAR, MUHAMMET KÖSE, AHMET KAYRALDIZ, and MÜKERREM KURTOĞLU

## Synthesis and X-ray powder diffraction, electrochemical, and genotoxic properties of a new azo-Schiff base and its metal complexes

Mustafa BAL<sup>1</sup>, Gökhan CEYHAN<sup>1</sup>, Barış AVAR<sup>2</sup>, Muhammet KÖSE<sup>1</sup>,  
Ahmet KAYRALDIZ<sup>3</sup>, Mükerrer KURTOĞLU<sup>1,\*</sup>

<sup>1</sup>Department of Chemistry, Faculty of Science and Arts, Kahramanmaraş Sütçü İmam University, Kahramanmaraş, Turkey

<sup>2</sup>Department of Metallurgy and Materials Engineering, Bülent Ecevit University, İncivez, Zonguldak

<sup>3</sup>Department of Biology, Faculty of Science and Arts, Kahramanmaraş Sütçü İmam University, Kahramanmaraş, Turkey

Received: 12.06.2013 • Accepted: 18.08.2013 • Published Online: 14.03.2014 • Printed: 11.04.2014

**Abstract:** A new, substituted 2-[(*E*)-{4-(benzyloxy)phenyl}imino} methyl]-4-[(*E*)-(4-nitrophenyl)diazenyl]phenol azo-azomethine ligand (mbH) was synthesized from 2-hydroxy-5-[(4-nitrophenyl)diazenyl]benzaldehyde and 4-benzyloxyanilinehydrochloride in ethyl alcohol solution. These mononuclear Mn(II), Co(II), Ni(II), Cu(II), and Zn(II) complexes of the ligand were prepared and their structures were proposed by elemental analysis, and infrared and ultraviolet-visible spectroscopy; the proton NMR spectrum of the mbH ligand was also recorded. The azo-azomethine ligand, mbH, behaves as a bidentate ligand coordinating through the nitrogen atom of the azomethine (–CH=N–) and the oxygen atom of the phenolic group. Elemental analyses indicated that the metal:ligand ratio was 1:2 in the metal chelates. Powder X-ray diffraction parameters suggested a monoclinic system for the mbH ligand and its Ni(II), Cu(II), Co(II), and Zn(II) complexes, and an orthorhombic system for the Mn(II) complex. Electrochemical properties of the ligand and its metal complexes were investigated in  $1 \times 10^{-3}$ – $1 \times 10^{-4}$  M DMF and CH<sub>3</sub>CN solvent in the range 200, 250, and 500 mV s<sup>-1</sup> scan rates. The ligand showed both reversible and irreversible processes at these scan rates. In addition, genotoxic properties of the ligand and its complexes were examined.

**Key words:** Azo dye, Schiff base, transition metal complexes, electrochemistry, X-ray powder diffraction, genotoxicity

### 1. Introduction

Schiff bases, first reported by Hugo Schiff in 1864, are condensation products of primary amines with carbonyl compounds.<sup>1</sup> The common structural feature of these compounds is the azomethine group with a general formula R–HC=N–R. These compounds are an important class of ligands in coordination chemistry and have found extensive application in various fields of science. d-Block metal complexes of Schiff bases have expanded enormously and embraced wide and diversified subjects comprising vast areas of organometallic compounds and various aspects of biocoordination chemistry.<sup>2–5</sup> A number of Schiff base derivatives have shown interesting biological activities such as antibacterial, antifungal, anticonvulsant, antimalarial, and anticancer.<sup>6–9</sup> Schiff base ligands and their metal complexes have also been investigated due to their interesting and important features, such as their ability to reversibly bind oxygen, and their use in catalyses for oxygenation and oxidation reactions of organic compounds and electrochemical reduction reactions.<sup>10–13</sup>

\*Correspondence: mkurtoglu@ksu.edu.tr

Azo dyes form an important class of organic colorants, consisting of at least a conjugated azo ( $-N=N-$ ) chromophore, and are the largest and most versatile class of dyes. Azo compounds have received considerable attention due to their impressive and useful chemical physical properties. These compounds belong to one of the most intensively studied groups for nonlinear optics, optical information storage, and optical switching.<sup>14–17</sup> Azo-azomethines have been extensively used as dyestuffs for wool, leather, and synthetic fabrics because of their extraordinary coloring properties and in photonic devices, electro-optic modulators, and components of optical communication systems due to their second-order nonlinear optical properties.<sup>18,19</sup>

Previously, we obtained and characterized various bidentate and/or polydentate ligands containing *N* and *O* donors.<sup>6,20–27</sup> In continuation of these studies, we discuss the synthesis of a new azo-azomethine ligand (mbH) and its mononuclear complexes with Mn(II), Co(II), Ni(II), Cu(II), and Zn(II). All the synthesized compounds were characterized by using various spectral (IR, <sup>1</sup>H NMR, and UV-Vis) and physico-chemical techniques. The elemental analysis, type of chelation of ligand, and the geometry of the metal complexes are discussed in detail.

## 2. Experimental

### 2.1. Chemicals

All reagents and solvents were purchased from commercial sources and used without further purification unless otherwise noted. 2-Hydroxy-5-[(*E*)-(4-nitrophenyl)diazenyl]benzaldehyde was prepared according to a previously published procedure.<sup>28</sup>

### 2.2. Physical measurements

Infrared spectra were obtained using KBr discs ( $4000-400\text{ cm}^{-1}$ ) on a PerkinElmer FT-IR spectrophotometer. The electronic absorption spectra of the compound in the 200–800 nm range were measured in DMSO on a T80+ UV-Vis spectrophotometer (PG Instruments Ltd). Carbon, hydrogen, and nitrogen elemental analyses were performed with a model LECO CHNS 932 elemental analyzer. <sup>1</sup>H NMR spectrum of the ligand was obtained in CDCl<sub>3</sub> as solvent on a Bruker FT-NMR AC-400 (400 MHz) spectrometer. All chemical shifts are reported in  $\delta$  (ppm) relative to the tetramethylsilane as internal standard. Powder X-ray diffraction analysis was performed by PANalytical X'Pert PRO instrument with Cu-K $\alpha$  radiation (wavelength 0.154 nm) operating at 40 kV and 30 mA. Measurements were scanned for diffraction angles ( $2\theta$ ) ranging from 20° to 90° with a step size of 0.02° and a time per step of 1 s. Melting points were obtained with a Electrothermal LDT 9200 apparatus in open capillaries. Cyclic voltammograms studies were recorded according to the literature method on an Iviumstat Electrochemical workstation equipped with a low current module (BAS PA-1) recorder.<sup>29</sup>

### 2.3. Synthesis of 2-[(*E*)-{4-(benzyloxy)phenyl}imino] methyl]-4-[(*E*)-(4-nitrophenyl)diazenyl]phenol, (mbH).1/2H<sub>2</sub>O

A solution of 4-benzyloxyanilinehydrochloride (433.50 mg, 2.176 mmol) in ethyl alcohol (10 mL) was mixed with a solution of 2-hydroxy-5-[(4-nitrophenyl)diazenyl]benzaldehyde (498.64 mg, 1.84 mmol) in ethyl alcohol (50 mL) and the reaction mixture was refluxed for 24 h. The dark yellow product formed was dissolved in ethyl alcohol (25 mL) and left for crystallization at room temperature for a day. Then orange crystals were collected, washed with cold ethyl alcohol, and dried in air. Yield, 650.00 mg (77%). Mp: 209–210 °C. Elemental analyses

for  $C_{26}H_{21}N_4O_{4.5}$  (461.46 g/mol): Found: C, 67.42; H, 4.34; N, 12.09%. Calcd.: C, 67.67; H, 4.59; N, 12.14%. IR ( $cm^{-1}$ ): 3448  $\nu$ (O–H hydrated water), 1637  $\nu$ (C=N), 1520  $\nu$ (–N=N–), 1342  $\nu$ (C=C), 1104  $\nu$ (C–O–C).

#### 2.4. Synthesis of di(aqua)bis{2-[(*E*)-{4-(benzyloxy)phenyl}imino} methyl]-4-[(*E*)-(4-nitrophenyl) diazenyl]phenolato} mangan(II), $[Mn(mb)_2(H_2O)_2] \cdot 4H_2O$

A solution of  $MnCl_2 \cdot 4H_2O$  (1.40 mg, 0.011 mmol) in methyl alcohol (10 mL) was added to a solution of mbH (10.00 mg, 0.022 mmol) in dichloromethane (20 mL). The mixture was then heated in a water bath for another 30 min to complete the precipitation. The red complex was filtered, washed with cold ethyl alcohol, and dried. Yield, 7.34 mg (64%). Mp: > 250 °C. Elemental analyses for  $C_{52}H_{50}MnN_8O_{14}$  (1065.93 g/mol): Found: C, 58.72; H, 3.90; N, 10.48%. Calcd.: C, 58.59; H, 4.73; N, 10.51%. IR ( $cm^{-1}$ ): 3419  $\nu$ (O–H hydrated water), 1630  $\nu$ (C=N), 1523  $\nu$ (–N=N–), 1342  $\nu$ (C=C), 1106  $\nu$ (C–O–C), 850 (coordinated water), ~650  $\nu$ (Mn–O), 545  $\nu$ (Mn–N).

#### 2.5. Synthesis of di(aqua)bis{2-[(*E*)-{4-(benzyloxy)phenyl}imino} methyl]-4-[(*E*)-(4-nitrophenyl) diazenyl]phenolato} nickel(II), $[Ni(mb)_2(H_2O)_2] \cdot 3H_2O$

2-[(*E*)-{4-(benzyloxy)phenyl}imino} methyl]-4-[(*E*)-(4-nitrophenyl)diazenyl]phenol ligand (10.00 mg, 0.022 mmol) was dissolved in dichloromethane (20 mL) at room temperature (Figure 1). A solution of  $NiCl_2 \cdot 6H_2O$  (2.70 mg, 0.011 mmol) in methyl alcohol (10 mL) was added dropwise into the solution of the ligand with continuous stirring. The mixture was refluxed for 3 h; the volume of the solution was then reduced to 10 mL and left to cool down to room temperature. On addition of ethyl alcohol (10 mL) a precipitate formed and

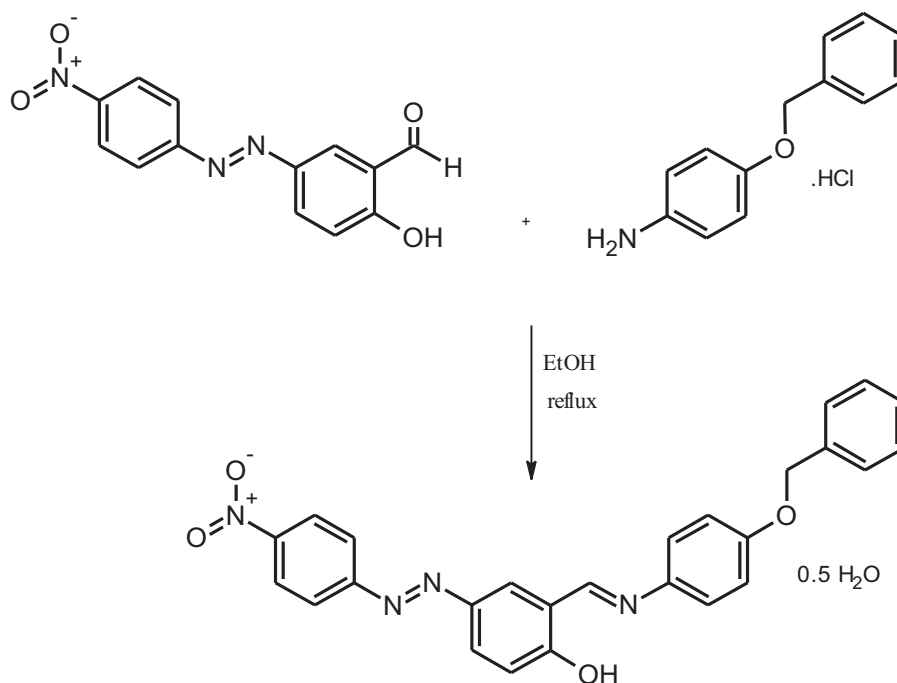


**Figure 1.** Synthesis of 2-[(*E*)-{4-(benzyloxy)phenyl}imino} methyl]-4-[(*E*)-(4-nitrophenyl)diazenyl]phenol (mbH).

was collected and washed with a small amount of ethyl alcohol. The orange product was recrystallized from hot ethyl alcohol and it was dried at room temperature. Yield, 8.00 mg (70%). Mp: 266–267 °C. Elemental analyses for  $C_{52}H_{48}N_8NiO_{13}$  (1051.67 g/mol): Found: C, 59.29; H, 4.00; N, 10.29%. Calcd.: C, 59.39; H, 4.60; N, 10.65%. IR ( $cm^{-1}$ ): 3409  $\nu$ (O–H hydrated water), 1627  $\nu$ (C=N), 1510  $\nu$ (–N=N–), 1376  $\nu$ (C=C), 1104  $\nu$ (C–O–C), 845 (coordinated water), 610  $\nu$ (Ni–O),  $\sim$ 540  $\nu$ (Ni–N).

## 2.6. Synthesis of di(aqua)bis{2-[(E)-{4-(benzyloxy)phenyl}imino] methyl}-4-[(E)-(4-nitrophenyl) diazenyl]phenolato} copper(II), $[Cu(mb)_2(H_2O)_2] \cdot 3H_2O$

$Cu(CH_3COO)_2 \cdot H_2O$  (2.20 mg, 0.011 mmol) was dissolved in methyl alcohol (10 mL) and stirred under reflux for 45 min, followed by the addition of the mbH Schiff base (10.00 mg, 0.022 mmol) in dichloromethane (20 mL), and the reaction mixture was refluxed for 3 h. The brown precipitate obtained was filtered, washed with methyl alcohol, and dried in air. Yield, 5.90 mg (51%). Mp: 250–251 °C. Elemental analyses for  $C_{52}H_{48}N_8CuO_{13}$  (1056.53 g/mol): Found: C, 58.43; H, 3.86; N, 10.52%. Calcd.: C, 59.11; H, 4.58; N, 10.61%. IR ( $cm^{-1}$ ): 3375  $\nu$ (O–H hydrated water), 1630  $\nu$ (C=N),  $\sim$ 1520  $\nu$ (–N=N–), 1340  $\nu$ (C=C), 1105  $\nu$ (C–O–C), 855 (coordinated water), 691  $\nu$ (Cu–O), 546  $\nu$ (Cu–N).

## 2.7. Synthesis of di(aqua)bis{2-[(E)-{4-(benzyloxy)phenyl}imino] methyl}-4-[(E)-(4-nitrophenyl) diazenyl]phenolato} cobalt(II), $[Co(mb)_2(H_2O)_2] \cdot 8H_2O$

A methanolic solution (10 mL) of  $Co(CH_3COO)_2 \cdot 4H_2O$  (2.60 g, 0.011 mmol) was added gradually to a dichloromethane solution (20 mL) of the ligand (10.00 mg, 0.022 mmol). The solution was stirred for 2 h and a reddish brown precipitate formed. The product was filtered and washed with ethyl alcohol and then diethyl ether, and finally dried in air. Yield, 7.40 mg (59%). Mp: 254 °C. Elemental analyses for  $C_{52}H_{58}CoN_8O_{18}$  (1141.99 g/mol): Found: C, 54.74; H, 4.70; N, 9.78%. Calcd.: C, 54.69; H, 5.12; N, 9.81%. IR ( $cm^{-1}$ ): 3390  $\nu$ (O–H/hydrated water), 1632  $\nu$ (C=N),  $\sim$ 1520  $\nu$ (–N=N–), 1342  $\nu$ (C=C), 1106  $\nu$ (C–O–C), 857 (coordinated water),  $\sim$ 650  $\nu$ (Co–O), 547  $\nu$ (Co–N).

## 2.8. Synthesis of di(aqua)bis{2-[(E)-{4-(benzyloxy)phenyl}imino] methyl}-4-[(E)-(4-nitrophenyl) diazenyl]phenolato} zinc(II), $[Zn(mb)_2(H_2O)_2] \cdot H_2O$

The red colored compound was prepared by the addition of  $Zn(CH_3COO)_2 \cdot 2H_2O$  (2.40 mg, 0.011 mmol) in methyl alcohol (10 mL) to a refluxing mixture of the ligand (10.00 mg, 0.022 mmol) mbH in dichloromethane (20 mL). The red compound was separated out via filtration, washed with cold ethyl alcohol, and dried in vacuo. Yield, 6.10 mg (55%). Mp: 286–287 °C. Elemental analyses for  $C_{52}H_{44}N_8O_{11}Zn$  (1022.36 g/mol): Found: C, 61.00; H, 3.83; N, 10.83%. Calcd.: C, 61.09; H, 4.34; N, 10.96%. IR ( $cm^{-1}$ ): 3395  $\nu$ (O–H hydrated water), 1625  $\nu$ (C=N),  $\sim$ 1515  $\nu$ (N=N), 1340  $\nu$ (C=C), 1103  $\nu$ (C–O–C), 845 (coordinated water), 698  $\nu$ (Zn–O), 545  $\nu$ (Zn–N).

## 2.9. Salmonella/microsome test (Ames)

### 2.9.1. Bacterial strains

Histidine deficient (his<sup>–</sup>) tester strains TA98 and TA100 of *Salmonella typhimurium* were provided by LK Nakamura (Microbiologist Emeritus, Microbial Properties Research, Department of Agriculture, Peoria, Illinois,

USA). The TA98 strain was used to detect the frameshift mutagens and the TA100 strain for the detection of base pair substitution mutagens. Each strain used for testing was checked for the presence of strain-specific marker as described by Maron and Ames.<sup>30</sup>

### 2.9.2. Mutagenicity assay and preparation of S9

The standard plate-incorporation assay was examined with *Salmonella typhimurium* TA98 and TA100 strains in the presence and absence of S9 mix according to Maron and Ames.<sup>30</sup> Mutagenicity tests and preparation of S9 for the compounds were performed according to the literature.<sup>30,31</sup> For the test, the mbH bidentate ligand and its metal complexes were dissolved in DMSO and used as 0.06, 0.12, 0.24, 0.49, and 0.98 mg per plate. Each sample was evaluated with 3 replicate plates and all tests were performed twice. Fresh S9 mix was used for each mutagenicity assay.

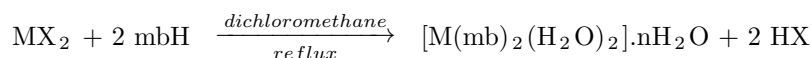
### 2.9.3. Statistical significance

The significance between control revertants and revertants of treated groups were also compared by t-test. Dose-response relationships were evaluated by using regression and correlation (r) test systems.

## 3. Results and discussion

### 3.1. Synthesis

2-[(*E*)-{4-(benzyloxy)phenyl}imino} methyl]-4-[(*E*)-(4-nitrophenyl)diazenyl]phenol (mbH) was prepared by the reaction of 2-hydroxy-5-[(4-nitrophenyl)diazenyl]benzaldehyde with 4-benzyloxyanilinehydrochloride in ethyl alcohol. The product of the condensation reaction of 2-hydroxy-5-[(4-nitrophenyl)diazenyl]benzaldehyde salt with 4-benzyloxyanilinehydrochloride is depicted in Figure 1. The new azo-azomethine ligand, 2-[(*E*)-{4-(benzyloxy)phenyl}imino} methyl]-4-[(*E*)-(4-nitrophenyl)diazenyl]phenol (mbH), resulted in mononuclear complexes (Figure 2) with Mn(II), Co(II), Ni(II), Cu(II), and Zn(II) as follows:



mbH: 2-[(*E*)-{4-(benzyloxy)phenyl}imino} methyl]-4-[(*E*)-(4-nitrophenyl)diazenyl]phenol

M = Mn(II) (n = 4); Co(II) (n = 8); Ni(II) (n = 3); Cu(II) (n = 3); Zn(II) (n = 1)

Experimental results of the elemental analyses of the synthesized ligand and its metal chelates are in good agreement with theoretical values. The elemental analyses of the complexes indicate that the metal-ligand ratios are 1:2 in the  $[\text{M}(\text{mb})_2(\text{H}_2\text{O})_2] \cdot n\text{H}_2\text{O}$  [M = Mn(II), n = 4; Co(II), n = 8; Ni(II), n = 3; Cu(II), n = 3; or Zn(II), n = 1] metal complexes. The purity of the compounds was checked by TLC using silica gel G as adsorbent. The ligand and its mononuclear complexes are not soluble in water. Single crystals of the new azo-azomethine ligand and its transition metal chelates could not be isolated from any organic solvent; thus, no definite structures could be described.

However, structures of the compounds were proposed based on the analytical and spectroscopic data as shown in Figures 1 and 2. The analytical and spectroscopic data showed that M(II) ions are 6-coordinate, bonded to 2 nitrogen (C=N) and 2 phenolic oxygen atoms of 2 azo-azomethine ligands and 2 water molecules. Coordination geometry around the metal centers is octahedral. M-N and M-O bonds are expected to be *trans* in

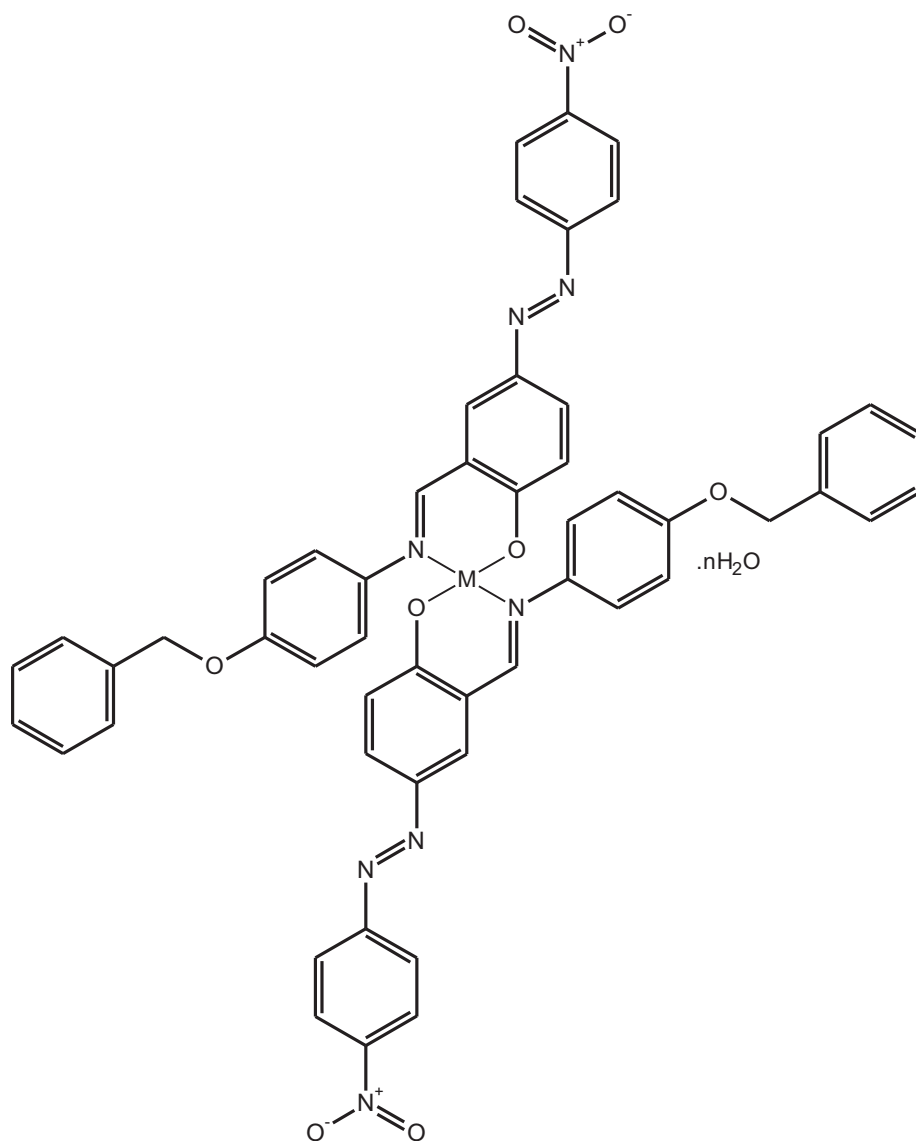


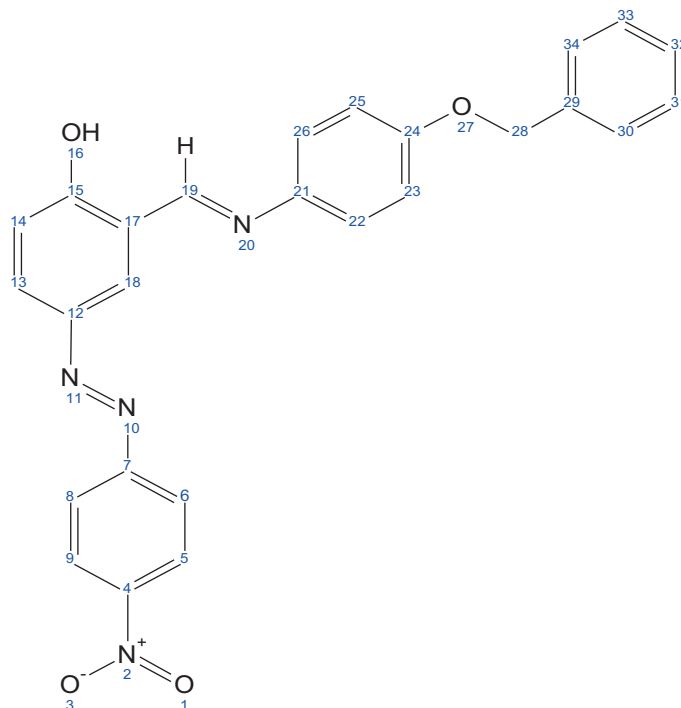
**Figure 2.** The proposed structure of metal complexes of the azo-azomethine ligand (mbH).

configuration due to steric reasons and this *trans* configuration was also observed for similar complexes reported in the literature.<sup>20–28</sup>

### 3.2. <sup>1</sup>H NMR spectrum of the ligand

For further information about the azo-azomethine ligand the <sup>1</sup>H NMR was recorded in CDCl<sub>3</sub>. NMR shifts of the ligand are shown in Table 1. The <sup>1</sup>H NMR spectrum confirms that the ligand is intact in solution. The hydrogen atom of the azomethine group (–CH=N–) was observed at δ 8.67 ppm as a singlet.<sup>6</sup> The aromatic protons were observed in the range of δ 6.98–8.67 ppm as a multiplet. Benzyl (C19) protons were assigned to a singlet peak at δ 5.05 ppm. A shift at δ 14.29 ppm could be assigned to phenolic proton (O(16)H).<sup>32</sup> Additionally, water protons were observed at 1.52 ppm. The presence of water in the structure was also confirmed by infrared spectroscopy and elemental analysis.



**Table 1.** The  $^1\text{H}$  NMR data (ppm) of the azo-azomethine (mbH) ligand in  $\text{CDCl}_3$ .

Chemical shifts, $\delta_{TMS}$ (ppm)	Assignments <sup>a</sup>	$J(\text{Hz})$
14.29	[s, 1H] (16)	-
8.67	[s, 1H] (19)	-
8.32	[d, 2H] (9, 5)	8.84
8.03	[d, 2H] (8, 6)	8.87
7.98	[s, 1H] (18)	-
7.92	[d, 1H] (13)	8.87
7.39	[d, 2H] (30, 34)	7.30
7.35	[t, 2H] (31, 33)	7.95
7.30	[t, 1H] (32)	8.81
7.27	[d, 1H] (14)	7.44
7.09	[d, 2H] (22, 26)	8.92
6.98	[d, 2H] (23, 25)	8.88
5.05	[s, 2H] (28)	-
1.52	[s, 2H] ( $\text{H}_2\text{O}$ )	-

<sup>a</sup>s: singlet; d: doublet and t: triplet.

### 3.3. FT-IR spectra

In order to study the bonding of the mbH azo-Schiff base to the metal, the infrared spectrum of the mbH was compared with spectra of the corresponding metal chelates. The infrared spectra provided valuable information regarding the nature of the functional groups attached to the metal ion. The main infrared bands and their assignments are given in the experimental section. In the spectrum of azo-azomethine ligand (mbH), a strong band at  $1637\text{ cm}^{-1}$  is attributed to the  $\text{C}=\text{N}$  (azomethine) group.<sup>33</sup> Upon coordination, this band  $\text{C}=\text{N}$  (azomethine) shifted to a lower frequency due to a shift of lone pair density toward the metal ion, indicating coordination of azomethine nitrogen to the metal center.<sup>34–36</sup> The spectrum of the mbH ligand exhibits a broad

band at  $3448\text{ cm}^{-1}$  due to phenolic and water  $-\text{OH}$ .<sup>37</sup> The phenolic  $-\text{OH}$  stretch disappears in the spectra of metal complexes, indicating that upon coordination of the ligand to metal centers the phenolic oxygen atoms are deprotonated. The spectra of the metal chelates exhibited broad bands at  $3448\text{--}3375\text{ cm}^{-1}$  that are attributed to OH of the crystal water molecules, while the bands observed at approximately  $857\text{--}845\text{ cm}^{-1}$  are assigned to coordinated water molecules.<sup>32,37</sup> A comparison between infrared spectra of mbH and the  $[\text{M}(\text{mb})_2]$  complexes also shows that a band, characteristic of  $\nu(\text{C}-\text{O})$  at  $1315\text{ cm}^{-1}$ , is shifted to  $1345\text{--}1325\text{ cm}^{-1}$ , due to  $\text{C}-\text{O}-\text{M}$  bond formation. Bands at  $2920\text{--}2885\text{ cm}^{-1}$  are assigned to  $\text{CH}_2$  asymmetric and symmetric stretching vibrations. The azo-Schiff base mbH showed a band at  $1342\text{ cm}^{-1}$  for  $\nu(\text{C}=\text{C})$  of aromatic rings, while its metal complexes shift to  $1376\text{--}1340\text{ cm}^{-1}$ . In addition, all the metal complexes show 2 new bands at  $698\text{--}610$  and  $547\text{--}540\text{ cm}^{-1}$  due to formation of  $\text{M}-\text{O}$  and  $\text{M}-\text{N}$  bonds, further confirming formation of coordination complexes.<sup>38</sup> All the vibrational data suggest that the metal ion bonded to the azo-azomethine ligand through the phenolic oxygen and the imino nitrogen atoms.

### 3.4. Electronic spectra

The electronic spectra of the mbH ligand and its metal chelates were recorded in DMSO between 200 and 800 nm. The compared dates of the UV-Vis spectra for the azo-azomethine dye and its metal chelates are shown in Table 2. The UV-Vis spectra of the ligand and its Ni(II) chelate in DMSO solution are shown in Figures 3 and 4.

**Table 2.** UV-Vis data of the ligand and its metal complexes in DMSO.

Compounds	$\lambda_{max}$ (nm)	Transitions
mbH	238, 292, 361	$\pi - \pi^*$ , $n - \pi^*$
$[\text{Mn}(\text{mb})_2(\text{H}_2\text{O})_2] \cdot 4\text{H}_2\text{O}$	234, 372, 535	$\pi - \pi^*$ , $n - \pi^*$ , d-d
$[\text{Co}(\text{mb})_2(\text{H}_2\text{O})_2] \cdot 8\text{H}_2\text{O}$	240, 391, 493	$\pi - \pi^*$ , $n - \pi^*$ , d-d
$[\text{Ni}(\text{mb})_2(\text{H}_2\text{O})_2] \cdot 3\text{H}_2\text{O}$	238, 314, 414, 516	$\pi - \pi^*$ , $n - \pi^*$ , d-d
$[\text{Cu}(\text{mb})_2(\text{H}_2\text{O})_2] \cdot 3\text{H}_2\text{O}$	237, 327, 531	$\pi - \pi^*$ , $n - \pi^*$ , d-d
$[\text{Zn}(\text{mb})_2(\text{H}_2\text{O})_2] \cdot \text{H}_2\text{O}$	240, 410, 540	$\pi - \pi^*$ , $n - \pi^*$ , CT

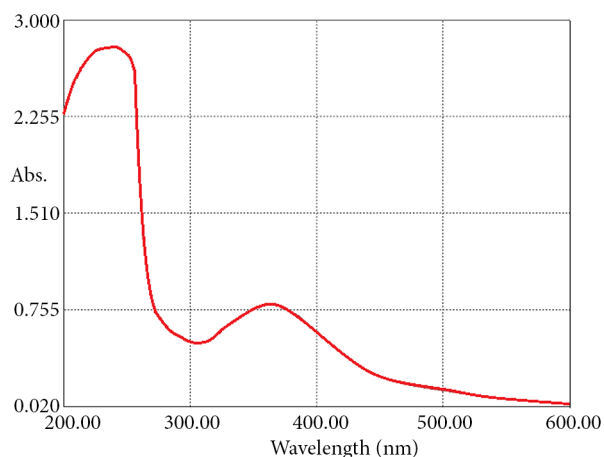


**Figure 3.** The UV-Vis spectrum of mbH.1/2H<sub>2</sub>O ligand in DMSO.

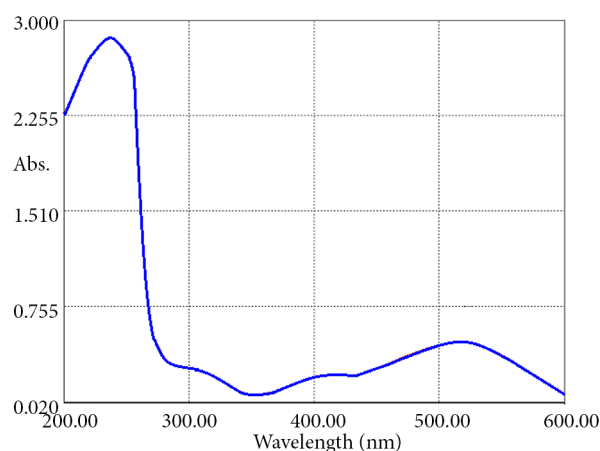


**Figure 4.** The UV-Vis spectrum of  $[\text{Ni}(\text{mb})_2(\text{H}_2\text{O})_2] \cdot 3\text{H}_2\text{O}$  complex in DMSO.

The absorption of the synthesized ligand (mbH) displays mainly 3 bands in DMSO solution at room temperature within the studied range. The band at 238 nm was assigned to the  $\pi \rightarrow \pi^*$  transition of aromatic rings, while the band at 292 nm as a shoulder is due to the low energy  $\pi \rightarrow \pi^*$  transition of the  $-\text{CH}=\text{N}-$  and  $-\text{N}=\text{N}-$  groups.<sup>39,40</sup> The peaks belonging to the  $\pi \rightarrow \pi^*$  transitions in the spectra of the  $[\text{Mn}(\text{mb})_2(\text{H}_2\text{O})_2] \cdot 4\text{H}_2\text{O}$ ,  $[\text{Ni}(\text{mb})_2(\text{H}_2\text{O})_2] \cdot 3\text{H}_2\text{O}$ ,  $[\text{Co}(\text{mb})_2(\text{H}_2\text{O})_2] \cdot 8\text{H}_2\text{O}$ ,  $[\text{Cu}(\text{mb})_2(\text{H}_2\text{O})_2] \cdot 3\text{H}_2\text{O}$ , and  $[\text{Zn}(\text{mb})_2(\text{H}_2\text{O})_2] \cdot \text{H}_2\text{O}$  coordination compounds were observed at 234, 238, 240, 237, and 240 nm, respectively. The band at 361 nm was assigned to the  $n \rightarrow \pi^*$  transitions of the  $-\text{CH}=\text{N}-$  and  $-\text{N}=\text{N}-$  azo chromophore groups. The peaks belonging to these groups in the spectra of the  $[\text{Mn}(\text{mb})_2(\text{H}_2\text{O})_2] \cdot 4\text{H}_2\text{O}$ ,  $[\text{Ni}(\text{mb})_2(\text{H}_2\text{O})_2] \cdot 3\text{H}_2\text{O}$ ,  $[\text{Co}(\text{mb})_2(\text{H}_2\text{O})_2] \cdot 8\text{H}_2\text{O}$ ,  $[\text{Cu}(\text{mb})_2(\text{H}_2\text{O})_2] \cdot 3\text{H}_2\text{O}$ , and  $[\text{Zn}(\text{mb})_2(\text{H}_2\text{O})_2] \cdot \text{H}_2\text{O}$  complexes appeared at 372, 314, 391, 327, and 410 nm, respectively. Furthermore, d-d transition bands in the spectra of the Mn(II), Co(II), Ni(II), and Cu(II) chelates were observed at 493–535 nm. The bands at 414 nm of Ni(II) and 540 nm of the Zn(II) chelates can be assigned to charge-transfer transitions. The spectroscopic data obtained in this work agreed well with those in previous work.<sup>41</sup>

### 3.5. X-ray powder diffraction analysis

Growth of single crystals of azo-azomethine compounds from various solvents including DMF, ethyl alcohol, chloroform etc. failed and so they were characterized by XRD.<sup>42,43</sup> X-ray powder diffraction analysis of the mbH ligand and its metal complexes was carried out to determine the type of crystal system, lattice parameters, and the cell volume. As shown in Figure 5 the XRD patterns indicate a crystalline nature for the mbH ligand and its metal complexes. Indexing of the diffraction patterns was performed using HighScore Plus software. For the Mn(II) and Co(II) complexes, for example, their Miller indices ( $hkl$ ) along with observed and calculated  $2\theta$  angles,  $d$  values, and relative intensities are given in Tables 3 and 4. From the indexed data the unit cell parameters were also calculated and are listed in Table 5. The powder XRD patterns of the compounds are completely different from those of the starting materials, demonstrating the formation of coordination compounds. It is found that mbH ligand and Ni(II), Cu(II), Co(II), and Zn(II) complexes have monoclinic structures, while Mn(II) complex has an orthorhombic structure. The crystal structures of similar type of samples were reported as monoclinic and orthorhombic.<sup>32,44–46</sup> Moreover, using the diffraction data, the mean crystallite sizes of the complexes,  $D$ , were determined according to the Scherrer equation ( $D = 0.9\lambda/(\beta \cos\theta)$ ), where  $\lambda$  is X-ray wavelength (1.5406 Å),  $\theta$  is Bragg diffraction angle, and  $\beta$  is the full width at half maximum of the diffraction peak).<sup>47,48</sup> The average crystallite sizes of all the samples were found to be  $\sim 38$ –75 nm and the values are given in Table 5.

### 3.6. Cyclic voltammograms

Cyclic voltammograms of the ligand and its complexes were run in DMF and  $\text{CH}_3\text{CN}$  solutions at room temperature using  $\text{Bu}_4\text{NBF}_4$  as supporting electrolyte at 293 K. All potentials quoted refer to measurements run at a scan rate ( $v$ ) of 200, 250, and 500  $\text{mV s}^{-1}$  and against an internal ferrocene–ferrocenium standard, unless otherwise stated. In order to investigate the effect of the ligand concentration, the electrochemical studies were performed in  $1 \times 10^{-3}$  and  $1 \times 10^{-4}$  M solutions of the ligand and its complexes. The voltammograms were recorded in the range from  $-2.0$  to  $2.0$  V vs.  $\text{Ag}^+/\text{AgCl}$ . The electrochemical data of the ligand and its complexes are summarized in Tables 6 and 7.

**Table 3.** XRD data of the  $[\text{Mn}(\text{mb})_2(\text{H}_2\text{O})_2] \cdot 4\text{H}_2\text{O}$  metal complex.

P.No.	<i>h</i>	<i>k</i>	<i>l</i>	2Th.(o) [°]	2Th.(c) [°]	d-sp.(o) [Å]	d-sp.(c) [Å]	Rel. Int. [%]
1	3	1	0	20.1641	20.164	4.400241	4.400274	100
2	3	0	1	21.2311	21.1882	4.181457	4.189827	12.16
3	2	0	2	23.9018	23.9011	3.719926	3.720043	19.32
4	0	3	1	25.8232	25.8256	3.447334	3.447019	72.06
5	4	1	1	28.0398	28.0364	3.179653	3.180032	33.54
6	3	1	2	28.8295	28.8319	3.094321	3.094069	33.93
7	0	0	3	30.5684	30.7969	2.922147	2.900988	47.85
8	3	3	1	31.9817	31.9846	2.796165	2.79592	77.6
9	5	0	1	32.8441	32.8522	2.724693	2.724033	31.54
10	3	1	3	37.0964	37.0892	2.421542	2.421999	58.66
11	0	4	2	38.1481	38.0359	2.357172	2.363864	35.51
12	6	2	0	41.0199	40.9886	2.198532	2.200137	44.13
13	3	4	2	42.6428	42.6343	2.118539	2.11894	46.76
14	3	1	4	46.5069	46.5263	1.951116	1.950348	8.07
15	3	2	4	48.6772	48.7038	1.869077	1.868118	12.73
16	7	1	2	49.8599	49.8176	1.827475	1.828927	18.46
17	8	0	0	50.837	50.8986	1.794621	1.792594	16
18	1	0	5	52.9586	52.9488	1.727614	1.727912	20.64
19	2	0	5	54.1668	54.1816	1.691897	1.69147	12.33
20	7	4	1	56.4883	56.5039	1.627748	1.627335	19.68
21	4	6	2	59.4269	59.458	1.55408	1.55334	7.77
22	6	0	5	66.4442	66.3865	1.405949	1.40703	12.96

**Table 4.** XRD data of the  $[\text{Co}(\text{mb})_2(\text{H}_2\text{O})_2] \cdot 8\text{H}_2\text{O}$  metal complex.

P.No.	<i>h</i>	<i>k</i>	<i>l</i>	2Th.(o) [°]	2Th.(c) [°]	d-sp.(o) [Å]	d-sp.(c) [Å]	Rel. Int. [%]
1	2	1	1	20.1819	20.1919	4.396392	4.394257	16.43
2	1	1	2	20.8981	20.8929	4.247317	4.248372	13.87
3	3	1	1	24.6466	24.6676	3.609173	3.606158	31.09
4	4	0	-3	25.7842	25.7678	3.452471	3.454619	100
5	1	1	-4	28.7745	28.7878	3.100117	3.098718	27.42
6	3	2	-1	31.676	31.6676	2.82245	2.823184	8.72
7	2	1	4	35.2553	35.2476	2.543671	2.544208	8.16

**Table 5.** XRD parameters of the mbH ligand and its metal complexes.

Sample	Lattice parameters				Volume (Å <sup>3</sup> )	Crystallite size <i>D</i> (nm)	Crystal system
	a (Å)	b (Å)	c (Å)	$\beta$ (°)			
(1) (mbH)	9.5494	15.4706	7.3935	98.0241	1081.5890	60	Monoclinic
(2) $[\text{Ni}(\text{mb})_2(\text{H}_2\text{O})_2] \cdot 3\text{H}_2\text{O}$	11.9487	3.9729	10.5231	100.6310	490.97	75	Monoclinic
(3) $[\text{Mn}(\text{mb})_2(\text{H}_2\text{O})_2] \cdot 4\text{H}_2\text{O}$	14.3386	11.2711	8.6961	90	1405.40	38	Orthorhombic
(4) $[\text{Cu}(\text{mb})_2(\text{H}_2\text{O})_2] \cdot 3\text{H}_2\text{O}$	13.4747	11.9007	10.1995	113.4330	1500.54	37	Monoclinic
(5) $[\text{Co}(\text{mb})_2(\text{H}_2\text{O})_2] \cdot 8\text{H}_2\text{O}$	15.8585	6.6875	14.0527	108.1620	1416.09	64	Monoclinic
(6) $[\text{Zn}(\text{mb})_2(\text{H}_2\text{O})_2] \cdot \text{H}_2\text{O}$	17.3896	8.5036	14.2796	120.0730	1827.34	52	Monoclinic

All complexes show strong cathodic peaks in the range from -0.5 to 1.0 V. The complexes have 2 anodic peaks in the 1.4–2.0 V range. The anodic and cathodic peaks are irreversible. The complexes show irreversible cathodic peak potentials in the 1.0–1.4 V range.

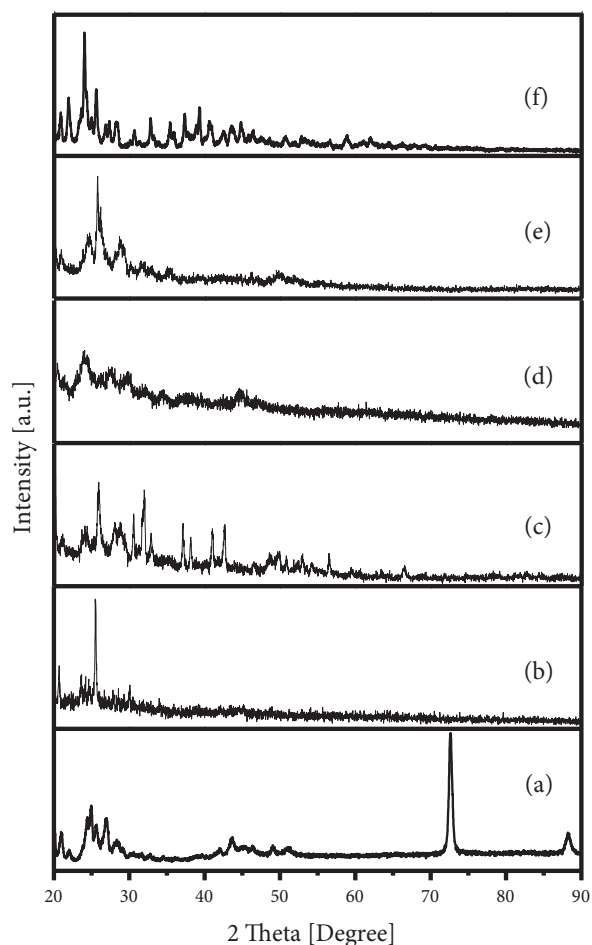


**Figure 5.** The XRD diffraction patterns of (a) (mbH), (b)  $[\text{Ni}(\text{mb})_2(\text{H}_2\text{O})_2] \cdot 3\text{H}_2\text{O}$ , (c)  $[\text{Mn}(\text{mb})_2(\text{H}_2\text{O})_2] \cdot 4\text{H}_2\text{O}$ , (d)  $[\text{Cu}(\text{mb})_2(\text{H}_2\text{O})_2] \cdot 3\text{H}_2\text{O}$ , (e)  $[\text{Co}(\text{mb})_2(\text{H}_2\text{O})_2] \cdot 8\text{H}_2\text{O}$ , and (f)  $[\text{Zn}(\text{mb})_2(\text{H}_2\text{O})_2] \cdot \text{H}_2\text{O}$ .

The  $[\text{Co}(\text{mb})(\text{H}_2\text{O})_2] \cdot 8\text{H}_2\text{O}$  complex shows the reversible process ( $I_{pa}:I_{pc} = 1.0$ ) in the  $1 \times 10^{-3}$  M DMF and  $\text{CH}_3\text{CN}$  solutions at the 250 and  $500 \text{ mV s}^{-1}$  scan rates. Their potential ranges change from 0.35 V to 1.28 V (Epc) and from 0.35 V to 1.34 V (Epa). The  $[\text{Cu}(\text{mb})(\text{H}_2\text{O})_2] \cdot 3\text{H}_2\text{O}$  complex shows the irreversible process ( $I_{pa}:I_{pc} \neq 1.0$ ) in the  $1 \times 10^{-3}$  M  $\text{CH}_3\text{CN}$  solution at the 250 and  $500 \text{ mV s}^{-1}$  scan rates. Their potential ranges change from  $-0.25$  V to 1.60 V (Epc) and from 0.21 V to 1.54 V (Epa). At the  $250 \text{ mV s}^{-1}$  scan rate, the  $[\text{Cu}(\text{mb})(\text{H}_2\text{O})_2] \cdot 3\text{H}_2\text{O}$  complex shows the reversible process ( $I_{pa}:I_{pc} \approx 1.0$ ) at 1.60 V (Epc) and 1.54 V (Epa). All processes at other potentials are irreversible in the  $1 \times 10^{-3}$  M  $\text{CH}_3\text{CN}$  and DMF solutions. The electrochemical curves of the  $[\text{Co}(\text{mb})(\text{H}_2\text{O})_2] \cdot 8\text{H}_2\text{O}$ ,  $[\text{Cu}(\text{mb})(\text{H}_2\text{O})_2] \cdot 3\text{H}_2\text{O}$ ,  $[\text{Mn}(\text{mb})(\text{H}_2\text{O})_2] \cdot 4\text{H}_2\text{O}$ ,  $[\text{Ni}(\text{mb})(\text{H}_2\text{O})_2] \cdot 3\text{H}_2\text{O}$ , and  $[\text{Zn}(\text{mb})(\text{H}_2\text{O})_2] \cdot \text{H}_2\text{O}$  complexes at 200, 250, and  $500 \text{ mV s}^{-1}$  scan rates in the  $1 \times 10^{-3}$  M DMF solutions are shown in Figures 6a–e.

The  $[\text{Mn}(\text{mb})(\text{H}_2\text{O})_2] \cdot 4\text{H}_2\text{O}$  complex shows the reversible process ( $I_{pa}:I_{pc} = 1.0$ ) in the  $1 \times 10^{-4}$  M  $\text{CH}_3\text{CN}$  solution at the  $500 \text{ mV s}^{-1}$  scan rate. Their potential ranges change from  $-1.35$  V to  $-0.76$  V (Epc) and from  $-1.35$  V to 0.61 V (Epa). The  $[\text{Mn}(\text{mb})(\text{H}_2\text{O})_2] \cdot 4\text{H}_2\text{O}$  complex show the irreversible process ( $I_{pa}:I_{pc} \neq 1.0$ ) in the  $1 \times 10^{-4}$  M DMF solution at the 250 and  $500 \text{ mV s}^{-1}$  scan rates. All processes at other potentials are irreversible in the  $1 \times 10^{-4}$  M  $\text{CH}_3\text{CN}$  and DMF solutions.

**Table 6.** Electrochemical data of the azo-Schiff base ligand and its metal complexes ( $1 \times 10^{-3}$  M).

Compound	Solvent	$E_{pa}$ (V)	$E_{pc}$ (V)	$E_{1/2}$ (mV)	$\Delta E_p$	$E_{pa}$ (V)	$E_{pc}$ (V)	$E_{1/2}$ (mV)	$\Delta E_p$	$E_{1/2}$ (mV)	$\Delta E_p$
mbH.1/2H <sub>2</sub> O	AN	-0.72, 0.29, 1.64	1.76, -0.62, -0.81	-	0.09	-0.69, 0.32, 0.84	1.47, -0.65, -1.09	-	-	-	0.33
	DMF	-1.12, -0.69, 1.01	-0.51, -0.90, -1.42	-	0.21	-1.11, -0.66, 1.05	-0.51, -0.90, -1.45	-	-	-	0.24
[Co(mb)(H <sub>2</sub> O) <sub>2</sub> ].8H <sub>2</sub> O	AN	0.35, 1.28	1.28, 0.90, 0.35	0.35*	0.38	0.30, 1.32	1.33, 0.89, 0.28	0.29*	-	-	0.23
	DMF	-0.60, 1.55	0.59, -0.65	0.62*	0.05	-0.65, 1.71	0.80, -0.71	-	-	-	0.06
[Cu(mb)(H <sub>2</sub> O) <sub>2</sub> ].3H <sub>2</sub> O	AN	-0.23, 0.36, 1.29	0.89, -0.10	-	0.40	-0.20, 0.31, 1.31	0.90, -0.12	-	-	-	0.40
	DMF	0.21, 0.82, 1.54	1.66, 1.12, -0.25	0.23*	0.46	0.20, 0.80, 1.50	1.64, 1.10, -0.20	-	-	-	0.40
[Mn(mb)(H <sub>2</sub> O) <sub>2</sub> ].4H <sub>2</sub> O	AN	-0.40, 1.68	1.31, -0.61	-	0.37	-0.31, 1.67	1.25, -0.62	-	-	-	0.42
	DMF	-0.59, 1.60	1.12, -0.69, -0.89	-	0.68	-0.50, 1.70	1.20, -0.70, -0.90	-	-	-	0.50
[Ni(mb)(H <sub>2</sub> O) <sub>2</sub> ].3H <sub>2</sub> O	AN	-0.70, 0.35	1.40, -0.40	-	0.95	-0.89, 0.30	1.31, 0.63	-	-	-	0.33
	DMF	-0.18, 1.70	1.23, -0.80	-	0.47	-0.20, 1.68	1.18, -0.84	-	-	-	0.70
[Zn(mb)(H <sub>2</sub> O) <sub>2</sub> ].H <sub>2</sub> O	AN	-0.90, 0.34, 1.78	1.21, -0.60, -1.09	-	0.56	-0.91, 0.35, 1.79	1.30, -0.62, -1.10	-	-	-	0.49
	DMF	-0.71, -0.38, 0.90	1.24, -0.63	-	0.25	-0.73, -0.20, 0.98	1.20, -0.70	0.71*	-	-	0.50

Supporting electrolyte: [NBu<sub>4</sub>](BF<sub>4</sub>) (0.1 M); concentrations of the compounds:  $1 \times 10^{-3}$  M. All the potentials are referenced to Ag<sup>+</sup>/AgCl, where  $E_{pa}$  and  $E_{pc}$  are anodic and cathodic potentials, respectively.  $E_{1/2} = 0.5 \times (E_{pa} + E_{pc})$ ,  $\Delta E_p = E_{pa} - E_{pc}$ . (i): These data have been obtained from scan rate  $250 \text{ mV s}^{-1}$ . Other data (ii) have been obtained by scan rate  $500 \text{ mV s}^{-1}$ . \*: Reversible

**Table 7.** Electrochemical data of the azo-Schiff base ligand and its metal complexes ( $1 \times 10^{-4}$  M).

Solvent	$E_{pa}$ (V)	$E_{pc}$ (V)	$E_{1/2}$ (mV)	$\Delta E_p$	$E_{pa}$ (V)	$E_{1/2}$ (mV)	$E_{pc}$ (V)	$\Delta E_p$	$E_{1/2}$ (mV)
mbH.1/2H <sub>2</sub> O	0.26, 0.76, 1.61	1.87	-	0.26	-1.43, -0.9, -0.3	-	1.82, -0.69, -0.88	0.39	-
	-0.97, -0.32, 1.5	-0.6, -1.31	-	0.28	-0.3	-	1.08	-	-
[Co(mb) <sub>2</sub> (H <sub>2</sub> O) <sub>2</sub> ].8H <sub>2</sub> O	-0.29, 0.23	-0.68, -1.03	-	0.39	-1.16, -0.89	-	1.57, -1.34	0.18	-
	-1.16, -0.89, 1.57	-1.34	-	0.18	-1.80, -0.86, 1.61	-	1.29, -0.61, -1.53	0.32	-
[Cu(mb) <sub>2</sub> (H <sub>2</sub> O)].3H <sub>2</sub> O	-0.33, 0.27, 1.28	-0.65, -1.14	-	0.33	-0.26, 1.28	-	-0.65, -1.17	0.39	-
	-0.42, 1.44	0.73, -0.62	0.52	0.20	-0.87, 0.96	0.52	1.27, -0.69, -1.56	0.69	-
[Mn(mb) <sub>2</sub> (H <sub>2</sub> O) <sub>2</sub> ].4H <sub>2</sub> O	-1.47, -0.85, -0.33	1.82, -0.68, -1.44	0.50	0.35	-1.35, 0.31, 0.61	0.50	-0.76, -1.35	-	1.00
	-1.09, -0.68, -0.33	1.29, -0.79, -1.24	-	0.11	-1.07, -0.6, 1.66	-	1.29	0.37	-
[Ni(mb) <sub>2</sub> (H <sub>2</sub> O) <sub>2</sub> ].3H <sub>2</sub> O	0.32, 1.66	1.87, 1.45	-	0.21	0.27, 1.63	-	1.87	-	-
	-0.3	-0.59	-	0.29	-0.34	-	-0.61	0.27	-
[Zn(mb) <sub>2</sub> (H <sub>2</sub> O) <sub>2</sub> ].H <sub>2</sub> O	-0.33, 0.32	1.43, -0.62	-	0.29	-0.32, 0.3, 1.62	-	1.79, -0.63, -1.1	0.31	-
	-0.36, 1.54	1.78, -0.6	-	0.24	-0.37, 1.58	-	-0.63, 1.24	0.26	0.50

Supporting electrolyte: [NBu<sub>4</sub>](BF<sub>4</sub>) (0.1 M); concentrations of the compounds:  $1 \times 10^{-4}$  M. All the potentials are referenced to Ag<sup>+</sup>/AgCl, where  $E_{pa}$  and  $E_{pc}$  are anodic and cathodic potentials, respectively.  $E_{1/2} = 0.5 \times (E_{pa} + E_{pc})$ ,  $\Delta E_p = E_{pa} - E_{pc}$ . (i): These data have been obtained from scan rate 250 mV s<sup>-1</sup>. Other data (ii) have been obtained by scan rate 500 mV s<sup>-1</sup>.

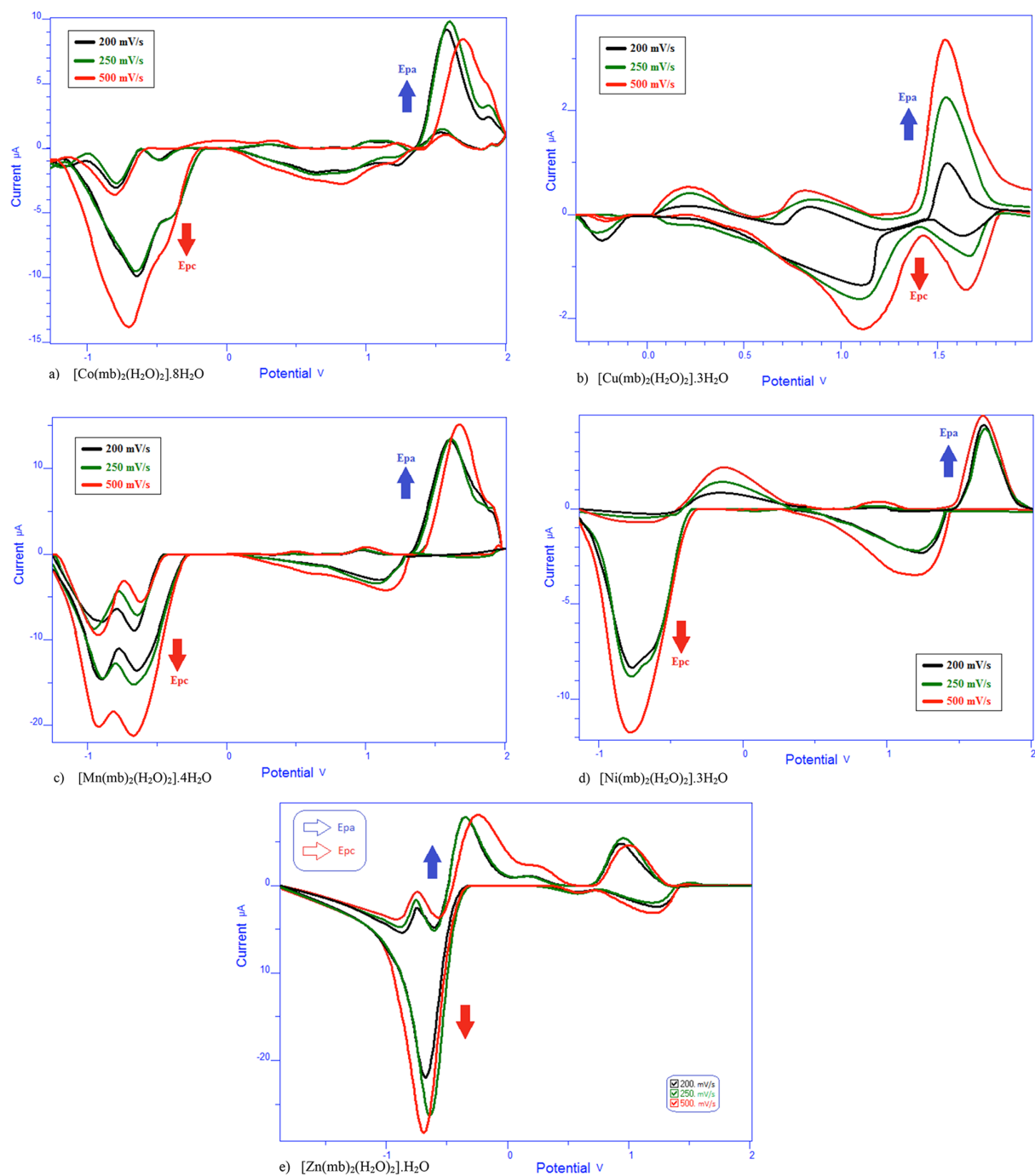


**Figure 6.** a–e The electrochemical curves of the metal complexes at 200, 250, and 500  $\text{mV s}^{-1}$  scan rates in DMF solution ( $1 \times 10^{-3}$  M).

The Zn(II) complex of the azo-Schiff base ligand mbH shows the reversible process at the  $-0.70$  V ( $E_{pc}$ ) and  $-0.73$  V ( $E_{pa}$ ) potentials at the  $500 \text{ mV s}^{-1}$  scan rate in the  $1 \times 10^{-3}$  M solution. The  $[\text{Zn}(\text{mb})_2(\text{H}_2\text{O})_2] \cdot \text{H}_2\text{O}$  chelate shows the reversible process at the  $-0.70$  and  $1.20$  V ( $E_{pc}$ ) and  $-0.73$ ,  $-0.20$ , and  $0.98$  V ( $E_{pa}$ ) potentials at the  $500 \text{ mV s}^{-1}$  scan rate in the  $1 \times 10^{-3}$  M solution. The  $[\text{Zn}(\text{mb})(\text{H}_2\text{O})_2] \cdot \text{H}_2\text{O}$



complex shows the irreversible process ( $I_{pa}:I_{pc} \neq 1.0$ ) in the  $1 \times 10^{-3}$  M and  $1 \times 10^{-4}$  M  $\text{CH}_3\text{CN}$  solutions at the 250 and 500  $\text{mV s}^{-1}$  scan rates. The electrochemical curves of the  $[\text{Co}(\text{mb})(\text{H}_2\text{O})_2] \cdot 8\text{H}_2\text{O}$ ,  $[\text{Cu}(\text{mb})(\text{H}_2\text{O})_2] \cdot 3\text{H}_2\text{O}$ ,  $[\text{Mn}(\text{mb})(\text{H}_2\text{O})_2] \cdot 4\text{H}_2\text{O}$ ,  $[\text{Ni}(\text{mb})(\text{H}_2\text{O})_2] \cdot 3\text{H}_2\text{O}$ , and  $[\text{Zn}(\text{mb})(\text{H}_2\text{O})_2] \cdot \text{H}_2\text{O}$  complexes at 200, 250, and 500  $\text{mV s}^{-1}$  scan rates in the  $1 \times 10^{-3}$  M  $\text{CH}_3\text{CN}$  solution are shown in Figures 7a–e.

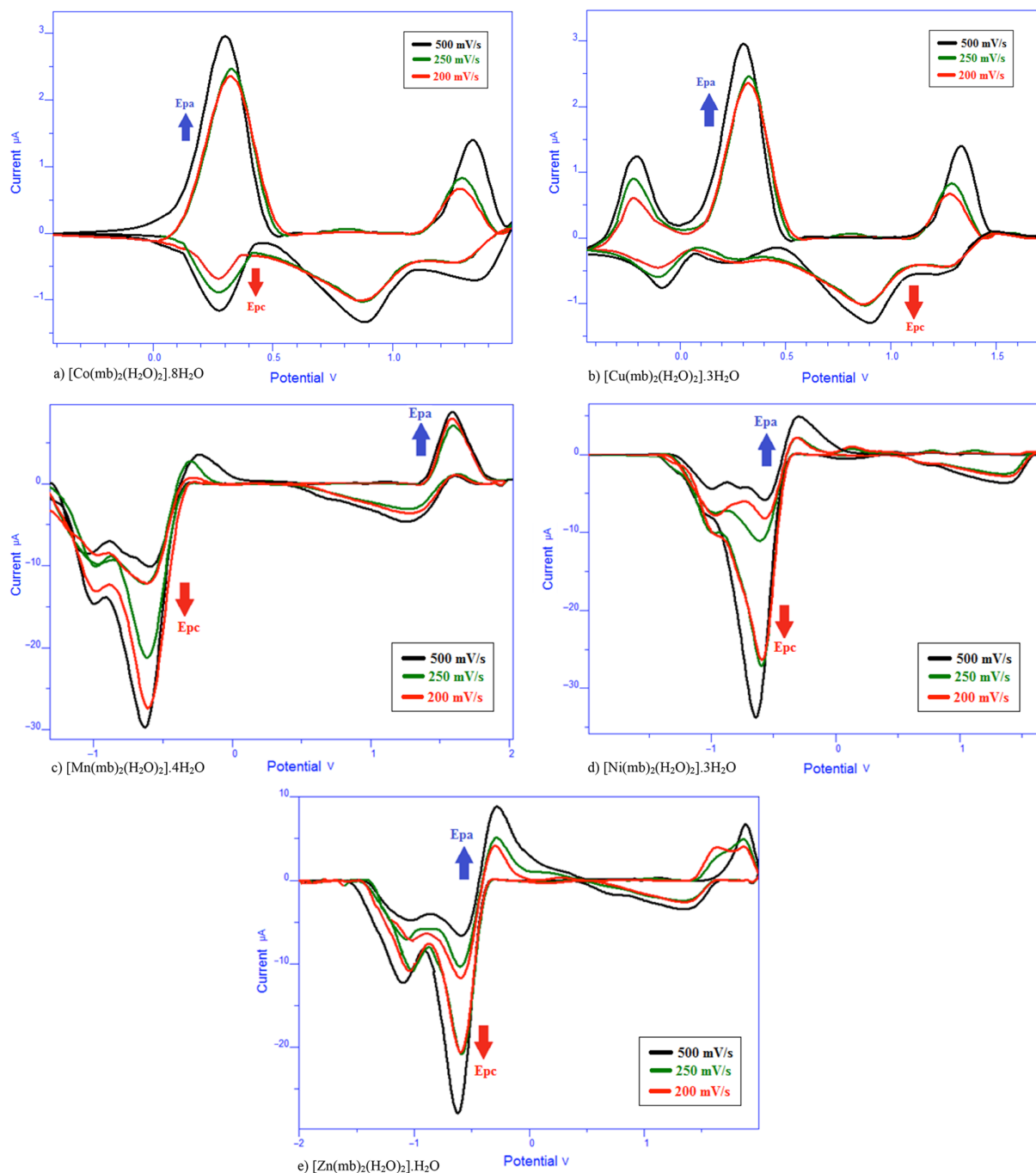
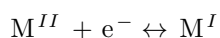


**Figure 7.** a–e The electrochemical curves of the metal complexes at 200, 250, and 500  $\text{mV s}^{-1}$  scan rates in  $\text{CH}_3\text{CN}$  solution ( $1 \times 10^{-3}$  M).

As the ligand has an electron donating benzyloxy group, the cathodic and anodic peak potentials were shifted to the negative regions. However, the ligand has a nitro group. As the nitro group has the electron accepting property, the redox potentials in the metal complexes shifted to the positive regions due to the  $-\text{NO}_2$  groups in the complexes, and the reduction and oxidation potentials were shifted to the higher positive regions.<sup>49</sup> The quinoid process would involve self-protonation reactions where the benzyloxy group acts as a proton donor. Oxidation–reduction peaks of the ligands at the different scan rates shifted to lower or higher potentials.<sup>45</sup> This process is shown below:



The mbH ligand showed the quinoid forms (Figure 8).

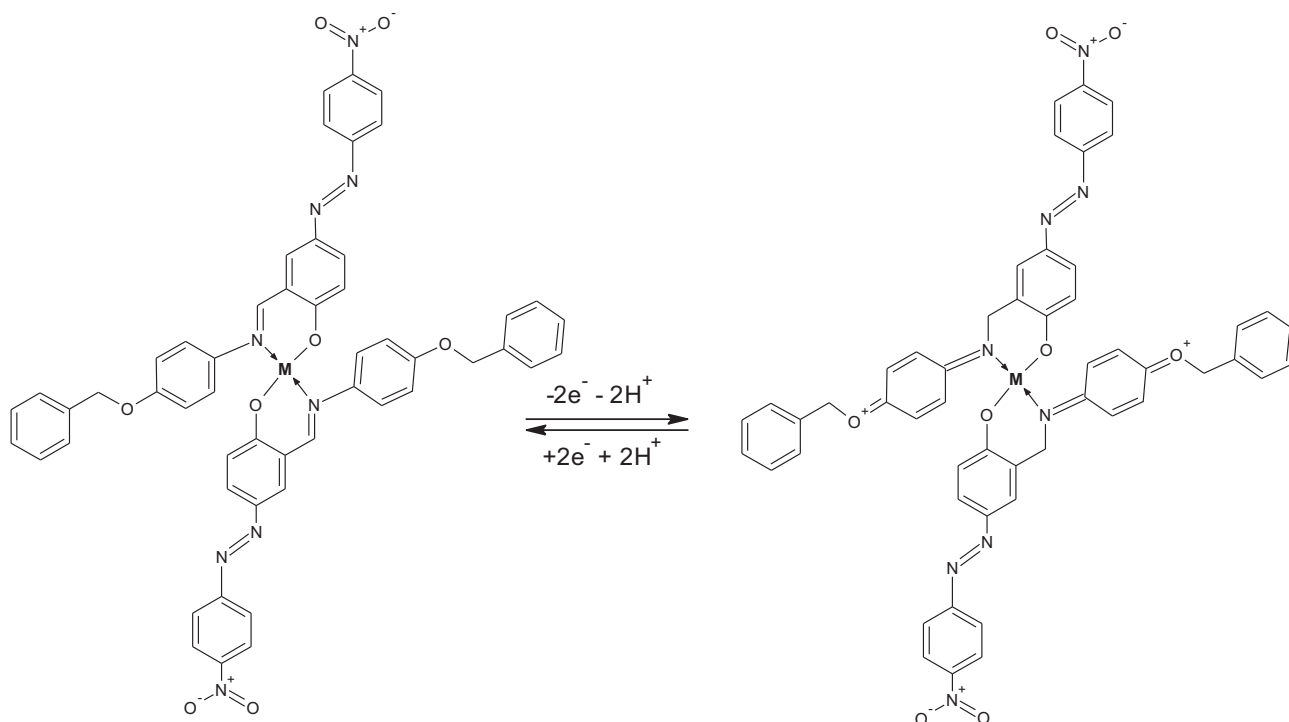


**Figure 8.** Reversible reduction–oxidation processes of the azo-Schiff base metal complexes in DMF solution.

### 3.7. Genotoxicity

The azo-azomethine (mbH) ligand was mutagenic on *S. typhimurium* TA98 but not mutagenic on *S. typhimurium* TA100 in the presence and absence of S9 mix (Table 8). In addition, mutagenic activity of the mbH ligand on TA98 increased with increasing dose in the presence and absence of S9 mix (Figure 9,  $r = 0.95924$ ; Figure 10,  $r = 0.96762$ ).

**Table 8.** The mutagenicity of mbH ligand and its metal complexes on *S. typhimurium* TA98 and TA100 in the presence or absence of S9 mix.

Test substances	Concentration mg/plate	TA98		TA100	
		- S9	+ S9	- S9	+ S9
Spontaneous control	-	10.50 ± 2.33	11.67 ± 2.51	106.7 ± 12.9	99.3 ± 10.1
4-NPD	200 $\theta$ g/mL				
2-AF	20 $\theta$ g/mL	3111 ± 225	3025 ± 172		691.0 ± 25.7
SA	1 $\theta$ g/mL			651.8 ± 48.5	
(1) mbH.1/2H <sub>2</sub> O	0.98	73.33 ± 4.03***	57.17 ± 5.22***	124.00 ± 5.77*	126.8 ± 16.4
	0.49	46.17 ± 3.50***	54.00 ± 6.58***	122.0 ± 19.7	116.3 ± 17.1
	0.24	40.83 ± 4.32***	34.33 ± 4.69**	101.50 ± 4.23	101.67 ± 6.11
	0.12	33.17 ± 4.74**	30.83 ± 4.78**	84.33 ± 3.57**	105.33 ± 4.52
	0.06	31.33 ± 3.51**	28.83 ± 3.65**	87.50 ± 13.2	71.17 ± 9.44*
(2) [Ni(mb) <sub>2</sub> (H <sub>2</sub> O) <sub>2</sub> ].3H <sub>2</sub> O	0.98	42.00 ± 3.54***	39.00 ± 5.14**	180.7 ± 21.5*	158.7 ± 18.2*
	0.49	32.50 ± 4.02**	34.83 ± 4.75**	141.0 ± 29.2	124.8 ± 12.2
	0.24	25.33 ± 2.56**	22.17 ± 3.24*	137.7 ± 18.6	111.3 ± 10.2
	0.12	20.00 ± 3.43*	18.50 ± 2.59*	112.7 ± 15.2	124.0 ± 20.4
	0.06	15.83 ± 1.97*	17.17 ± 2.99	79.83 ± 6.67**	91.8 ± 12.3
(3) [Mn(mb) <sub>2</sub> (H <sub>2</sub> O) <sub>2</sub> ].4H <sub>2</sub> O	0.98	27.17 ± 2.57***	27.33 ± 3.19**	127.00 ± 4.12**	122.00 ± 5.28**
	0.49	25.67 ± 1.82***	32.17 ± 1.76***	132.00 ± 7.82*	133.00 ± 8.04**
	0.24	20.50 ± 1.65***	20.55 ± 1.84**	117.8 ± 9.9	106.83 ± 7.35
	0.12	14.33 ± 2.06	14.83 ± 3.35	107.33 ± 9.06	112.0 ± 10.5
	0.06	13.00 ± 1.98	12.50 ± 1.61	78.81 ± 6.18**	85.83 ± 9.46
(4) [Cu(mb) <sub>2</sub> (H <sub>2</sub> O) <sub>2</sub> ].3H <sub>2</sub> O	0.98	29.00 ± 3.39**	28.83 ± 4.30**	120.67 ± 6.96	114.0 ± 5.74
	0.49	31.33 ± 3.36**	32.50 ± 4.15**	111.3 ± 13.8	103.0 ± 6.66
	0.24	26.83 ± 2.98**	27.17 ± 3.41**	97.33 ± 5.41	94.33 ± 6.26
	0.12	21.67 ± 2.30**	18.83 ± 2.50*	76.17 ± 5.16*	74.00 ± 5.74**
	0.06	17.67 ± 2.63*	18.67 ± 2.26*	54.67 ± 4.55***	58.50 ± 8.13**
(5) [Co(mb) <sub>2</sub> (H <sub>2</sub> O) <sub>2</sub> ].8H <sub>2</sub> O	0.98	114.33 ± 7.49***	110.17 ± 7.40***	213.7 ± 36.3**	164.2 ± 36.8*
	0.49	100.33 ± 9.78***	110.67 ± 9.81***	162.5 ± 27.4*	222.8 ± 36.3**
	0.24	67.3 ± 11.6**	84.7 ± 10.5***	123.2 ± 15.0	158.8 ± 30.9*
	0.12	61.00 ± 9.65**	68.2 ± 13.3**	117.3 ± 19.8	151.0 ± 32.0
	0.06	33.17 ± 7.13*	45.0 ± 10.2*	78.67 ± 6.90**	97.0 ± 13.2
(6) [Zn(mb) <sub>2</sub> (H <sub>2</sub> O) <sub>2</sub> ].H <sub>2</sub> O	0.98	36.33 ± 1.78***	36.83 ± 2.33***	121.17 ± 6.32	106.00 ± 7.35
	0.49	28.33 ± 5.17*	31.67 ± 4.60**	90.33 ± 3.99**	95.17 ± 7.11
	0.24	15.33 ± 1.23*	21.33 ± 2.70*	93.50 ± 7.98	93.17 ± 5.51
	0.12	19.33 ± 2.54*	19.00 ± 1.81**	74.0 ± 10.3*	76.50 ± 5.79*
	0.06	14.33 ± 3.28	15.00 ± 2.37	59.00 ± 5.99***	67.2 ± 10.9*

\*: P &lt; 0.05; \*\*: P &lt; 0.01; \*\*\*: P &lt; 0.001

NPD: 4-nitro-o-phenylenediamine, 2AF: 2-Aminofluorene, SA: Sodium azide

Similarly, Cu(II), Ni(II), and Zn(II) metal complexes of (mbH) ligand [(4)[Cu(mb)<sub>2</sub>(H<sub>2</sub>O)<sub>2</sub>].3H<sub>2</sub>O, (2)[Ni(mb)<sub>2</sub>(H<sub>2</sub>O)<sub>2</sub>].3H<sub>2</sub>O, and (6)[Zn(mb)<sub>2</sub>(H<sub>2</sub>O)<sub>2</sub>].H<sub>2</sub>O] were also mutagenic on *S. typhimurium* TA98 but not mutagenic on *S. typhimurium* TA100 in the absence or presence of S9 mix. In addition, mutagenic activity of (2)[Ni(mb)<sub>2</sub>(H<sub>2</sub>O)<sub>2</sub>].3H<sub>2</sub>O on *S. typhimurium* TA98 increased with increasing dose in the presence or absence of S9 mix (Figure 9, r = 0.98882; Figure 10, r = 0.95068) and mutagenic activity of (6)[Zn(mb)<sub>2</sub>(H<sub>2</sub>O)<sub>2</sub>].H<sub>2</sub>O on *S. typhimurium* TA98 increased with increasing dose in the presence of S9 mix (Figure 10, r = 0.97699).

Co(II) and Mn(II) metal complexes of (mbH) ligand [(5)[Co(mb)<sub>2</sub>(H<sub>2</sub>O)<sub>2</sub>].8H<sub>2</sub>O, (3)[Mn(mb)<sub>2</sub>(H<sub>2</sub>O)<sub>2</sub>].4H<sub>2</sub>O] exerted strong mutagenic activity on *S. typhimurium* TA98 but weak mutagenic activity on *S. typhimurium* TA100 in the absence or presence of S9 mix. Moreover, mutagenic activity of (5)[Co(mb)<sub>2</sub>(H<sub>2</sub>O)<sub>2</sub>].8H<sub>2</sub>O and (3)[Mn(mb)<sub>2</sub>(H<sub>2</sub>O)<sub>2</sub>].4H<sub>2</sub>O on *S. typhimurium* TA98 increased with increasing dose in the absence or S9 mix (Figure 9, r = 0.99735; Figure 10, r = 0.9768).

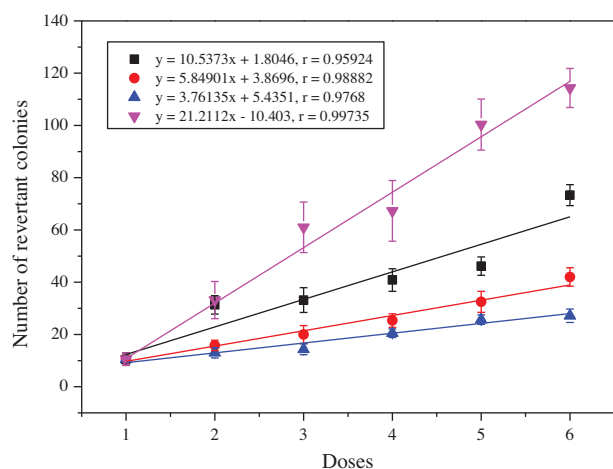


**Figure 9.** Dose-dependent increase in the mutagenic activity of (mbH) ligand and its metal complexes on *S. typhimurium* TA98 in the absence of S9 mix. Square, circle, triangle and upside down triangle represent, respectively, (mbH) ligand, [Ni(mb)<sub>2</sub>(H<sub>2</sub>O)<sub>2</sub>].3H<sub>2</sub>O, [Mn(mb)<sub>2</sub>(H<sub>2</sub>O)<sub>2</sub>].4H<sub>2</sub>O, and [Cu(mb)<sub>2</sub>(H<sub>2</sub>O)<sub>2</sub>].3H<sub>2</sub>O.

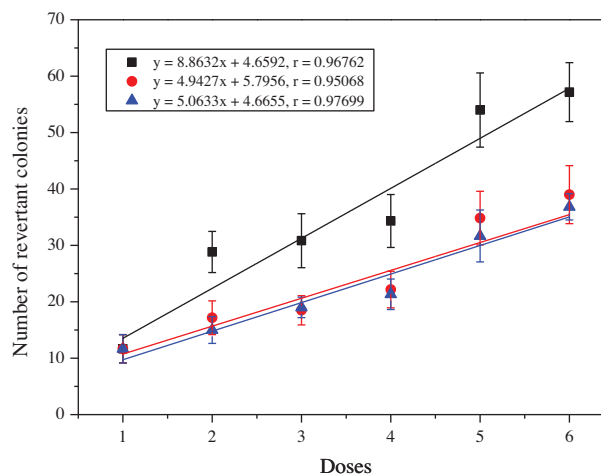


**Figure 10.** Dose dependent increase in the mutagenic activity of mbH ligand and its metal complexes on *S. typhimurium* TA98 in the presence of S9 mix. Square, circle, and triangle represent, respectively, mbH ligand, [Ni(mb)<sub>2</sub>(H<sub>2</sub>O)<sub>2</sub>].3H<sub>2</sub>O, and [Zn(mb)<sub>2</sub>(H<sub>2</sub>O)<sub>2</sub>].H<sub>2</sub>O.

#### 4. Conclusion

In this work an azo chromophore group containing a Schiff base ligand, 2-[(*E*)-{4-(benzyloxy)phenyl}imino}methyl]-4-[(*E*)-(4-nitrophenyl)diazenyl]phenol derived from 2-hydroxy-5-[(4-nitrophenyl)diazenyl]benzaldehyde with 4-benzyloxyaniline hydrochloride in ethyl alcohol and some of its transition metal complexes were prepared. The analytical data and the spectroscopic studies suggested that the complexes had the general formula [M(mb)<sub>2</sub>(H<sub>2</sub>O)<sub>2</sub>].nH<sub>2</sub>O, where M is manganese(II), cobalt(II), nickel(II), copper(II), or zinc(II). According to the UV-Vis and IR data of the nitrophenylazo linked Schiff base ligand, mbH was coordinated to the metal ion through the azomethine nitrogen (-CH=N-) and phenolic oxygen atom. From the XRD results, it was found that the mbH ligand and Ni(II), Cu(II), Co(II), and Zn(II) complexes have monoclinic structures, while the Mn(II) complex has a orthorhombic structure. In the electrochemical studies of the ligand and its metal chelates, reversible and irreversible redox processes were shown. Based on the above results, the structure of the coordination compounds under investigation can be formulated as in Figure 2.

According to data obtained from the salmonella/microsome test, the mbH ligand and its 5 transition metal complexes tested and their metabolites induced frameshift mutation (TA98). Generally, the effect of the mbH azo-azomethine ligand and its complexes on TA98 was greater than that on TA100.

#### Acknowledgments

This work was supported by the KSU Research Fund (No: 2010/2-22YLS). The authors wish to express their thanks to Prof Musa Göğebakan for the use of the X-ray diffractometer, and Prof Mehmet Tümer for electrochemistry measurements and his valuable discussion.

## References

1. Schiff, H. *Ann. Chem.* **1864**, *131*, 118–119.
2. Trujillo, A.; Fuentealba, M.; Carrillo, D.; Ledoux-Rak, I.; Hamon, J. R.; Saillard, J. Y. *Inorg. Chem.* **2010**, *49*, 2750–2764.
3. Fuentealba, M.; Garland, M. T.; Carrillo, D.; Manzur, C.; Hamon, J. R.; Saillard, J. Y. *Dalton Trans.* **2008**, *49*, 77–86.
4. Osinsky, S. P.; Levitin, I. Y.; Sigan, A. L.; Bubnovskaya, L. N.; Ganusevich, I. I.; Campanella, L.; Wardman, P. *Russ. Chem. Bull.* **2003**, *52*, 2636–2645.
5. Beinert, H.; Kennedy, M. C.; Stout, C. D. *Chem. Rev.* **1996**, *96*, 2335–2374.
6. Kurtoglu, M.; Ispir, E.; Kurtoglu N.; Serin, S. *Dyes Pigments* **2008**, *77*, 75–80.
7. Dimiza, F.; Papadopoulos, A. N.; Tangoulis, V.; Psycharis, V.; Raptopoulou, C. P.; Kessissoglou, D. P.; Psomas, G. *Dalton Trans.* **2010**, *39*, 4517–4528.
8. Harpstrite, S. E.; Collins, S. D.; Oksman, A.; Goldberg, D. E.; Sharma, V. *Med. Chem.* **2008**, *4*, 392–395.
9. Abd-Elzaher, M. M.; Moustafa, S. A.; Labib, A. A.; Ali, M. M. *Monatsh. Chem.* **2010**, *141*, 387–393.
10. Park, S.; Mathur, V. K.; Planap, R. P. *Polyhedron* **1998**, *17*, 325–330.
11. Nashinaga, A.; Ohara, H.; Tomita, H.; Matsuura, T. *Tetrahedron Lett.* **1983**, *24*, 213–216.
12. Pletcher, D.; Thompson, H. *J. Electroanal. Chem.* **1999**, *464*, 168–175.
13. Kianfara, A. H.; Paliz, M.; Roushani, M.; Shamsipur, M. *Spectrochim. Acta A* **2011**, *82*, 44–48.
14. Ho, M. S.; Barrett, C.; Paterson, J.; Esteghamatian, M.; Natansohn, A.; Rochon, P. *Macromolecules* **1996**, *29*, 4613–4618.
15. Yin, S.; Xu, H.; Shi, W.; Gao, Y.; Song, Y.; Wing, J. *Polymer* **2005**, *46*, 7670–7677.
16. Ho, M. S.; Natansohn, A. *Macromolecules* **1995**, *28*, 6124–6127.
17. Nabeshima, Y.; Shishido, A.; Kanazawa, A.; Shiono, T.; Ikeda, T.; Hiyama, T. *Chem. Mater.* **1997**, *9*, 1480–1487.
18. Kamel, M.; Galil, F.; Abdelwahab, L.; Osman, A. J. *Prakt. Chem.* **1971**, *313*, 1011–1021.
19. Gopal, J.; Srinivasan, M. J. *Polym. Sci. Polym. Chem. Ed.* **1986**, *24*, 2789–2796.
20. Serin, S.; Kurtoglu, M. *Analyst* **1994**, *119*, 2213–2215.
21. Kurtoglu, M.; Birbicer, N.; Kimyonsen, U.; Serin, S. *Dyes Pigments* **1999**, *41*, 141–143.
22. Birbicer, N.; Kurtoglu, M.; Serin, S. *Synth. React. Inorg. Met. Org. Chem.* **1999**, *29*, 1353–1364.
23. Kurtoglu, N.; Kurtoglu, M.; Serin, S. *Synth. React. Inorg. Met. Org. Chem.* **1999**, *29*, 1779–1791.
24. Kurtoglu, M.; Serin, S. *Synth. React. Inorg. Met. Org. Chem.* **2001**, *31*, 1129–1139.
25. Kurtoglu, M. *Synth. React. Inorg. Met. Org. Chem.* **2004**, *34*, 967–977.
26. Kurtoglu, M.; Baydemir, S. A. *J. Coord. Chem.* **2007**, *60*, 655–665.
27. Kurtoglu, M.; Serin, S. *Synth. React. Inorg. Met. Org. Chem.* **2002**, *32*, 629–637.
28. Khanmohammadi, H.; Darvishpour, M. *Dyes Pigments* **2009**, *81*, 167–173.
29. Ceyhan, G.; Kose, M.; McKee, V. *J. Lumin.* **2012**, *132*, 850–857.
30. Maron, D. M.; Ames, B. N. *Mutation Research* **1983**, *113*, 173–215.
31. Bal, M. Master's Thesis, Institute of Science, KSU, 2010, Kahramanmaraş, Turkey.
32. Kara, Y.; Avar, B.; Kayraldiz, A.; Güzel, B.; Kurtoglu, M. *Heteroatom Chem.* **2011**, *22*, 119–130.
33. Karipcin, F.; Dede, B.; Ozkorucuklu, S. P.; Kabalcilar, E. *Dyes Pigments* **2010**, *84*, 14–18.
34. Gulcan, M.; Sonmez, M.; Berber, I. *Turk. J. Chem.* **2012**, *36*, 189–200.
35. Halli, M. B.; Patil, V. B.; Bevinamarada, S. R. *Turk. J. Chem.* **2011**, *35*, 393–404.

36. Kulaksizoglu, S.; Gokce, C.; Gup, R. *Turk. J. Chem.* **2012**, *36*, 717–733.
37. Alghool, S.; Hanan, S. A.; El-Halim, F. A.; Dahshan, A. *J. Mol. Struct.* **2010**, *983*, 32–38.
38. Ispir, E. *Dyes Pigments* **2009**, *82*, 13–19.
39. Khedr, A. M.; Gaber, M.; Issa, R. M.; Erten, H. *Dyes Pigments* **2005**, *67*, 117–126.
40. Kurtoglu, N. *J. Serb. Chem. Soc.* **2009**, *74*, 917–926.
41. Kilincarslan, R.; Erdem, E.; Kocaokutgen, H. *Trans. Met. Chem.* **2007**, *32*, 102–106.
42. Chavan, S. S.; Sawant, V. A. *J. Mol. Struct.* **2010**, *965*, 1–6.
43. Ide, S.; Ancin, N.; Oztas, S. G.; Tuzun, M. *J. Mol. Struct.* **2001**, *562*, 1–9.
44. Joseph, J.; Mehta, B. H. *J. Coord. Chem.* **2007**, *33*, 124–129.
45. Roy, G. B. *Inorg. Chim. Acta* **2009**, *362*, 1709–1714.
46. Munde, A. S.; Jagdale, A. N.; Jadhav, S. M.; Chondhekar, T. K. *J. Serb. Chem. Soc.* **2010**, *75*, 349–359.
47. Baranwal, B. P.; Fatma, T.; Varma, A. *J. Mol. Struct.* **2009**, *920*, 472–477.
48. Kolmas, J.; Jaklewicz, A.; Zima, A.; Bucko, M.; Paszkiewicz, Z.; Lis, J.; Sloarczyk, A.; Kolodziejcki, W. *J. Mol. Struct.* **2011**, *987*, 40–50.
49. Ceyhan, G.; Celik, C.; Urus, S.; Demirtaş, I.; Elmastas, M.; Tumer, M. *Spectrochim. Acta A* **2011**, *81*, 184–198.